Muscle Synergies Encoded Within the Spinal Cord: Evidence From Focal Intraspinal NMDA Iontophoresis in the Frog

PHILIPPE SALTIEL, KUNO WYLER-DUDA, ANDREA D'AVELLA, MATTHEW C. TRESCH, AND EMILIO BIZZI

Department of Brain and Cognitive Sciences, Massachusetts Institute of Technology, Cambridge, Massachusetts 02139

Received 20 June 2000; accepted in final form 24 October 2000

Saltiel, Philippe, Kuno Wyler-Duda, Andrea d'Avella, Matthew C. Tresch, and Emilio Bizzi. Muscle synergies encoded within the spinal cord: evidence from focal intraspinal NMDA iontophoresis in the frog. *J Neurophysiol* 85: 605–619, 2001. This paper relates to the problem of the existence of muscle synergies, that is whether the CNS command to muscles is simplified by controlling their activity in subgroups or synergies, rather than individually. We approach this problem with two methods that have been recently introduced: intraspinal *N*-methyl-D-aspartate (NMDA) microstimulation and a synergy-extracting algorithm. To search for a common set of synergies encoded for by the spinal cord whose combinations would account for a large range of electromyographic (EMG) patterns, we chose, rather than examining a large range of natural behaviors, to chemically microstimulate a large number of spinal cord interneuronal sites in different frogs. A possible advantage of this complementary method is that it is task-independent. Visual inspection suggested that the NMDA-elicited EMG patterns recorded from 12 leg muscles might indeed be constructed from smaller subgroups of muscles whose activity co-varied, suggestive of synergies. We used a modification of our extracting computational algorithm whereby a nonnegative least-squares method was employed to iteratively update both the synergies and their coefficients of activation in reconstructing the EMG patterns. Using this algorithm, a limited set of seven synergies was found whose linear combinations accounted for more than 91% of the variance in the pooled EMG data from 10 frogs, and more than 96% in individual frogs. The extracted synergies were similar among frogs. Further, preferred combinations of these synergies were clearly identified. This was found by extracting smaller sets of four, five, or six synergies and fitting each synergy from those sets as a combination from the set of seven synergies extracted from the same frog; the synergy combinations from each frog were then pooled together to examine their frequency of occurrence. Concordance with this method of identifying synergy combinations was found by examining how the synergies from the set of seven correlated pair-wise as they reconstructed the EMG data. These results support the existence of muscle synergies encoded within the spinal cord, which through preferred combinations, account for a large repertoire of spinal cord motor output. These findings are contrasted with previous approaches to the problem of synergies.

INTRODUCTION

A central problem in motor physiology is how the activity of many muscles is coordinated to produce movement. The multiarticular nature of the limb and its large number of muscles together imply many available degrees of freedom to accomplish motor tasks (Bernstein 1967). While this redundancy provides flexibility, it appears that generally the CNS utilizes preferred ways to achieve a given task. Indeed, a number of task-dependent constraints have been identified as invariant kinematic features (Grasso et al. 1998; Lacquaniti and Soechting 1982; Santello et al. 1998; Soechting et al. 1986). Besides interaction torques between limb segments, some type of muscle coordination is crucial in determining these kinematics. Given that the CNS output is motoneuronal, it has been suggested that the reduction of the number of degrees of freedom and muscle coordination could both arise through the control of muscles as groups or synergies, rather than individually. This would have important implications for the neural circuitry (Soechting and Lacquaniti 1989).

In the present study, we are seeking to identify whether such synergies exist. The framework we chose is to define a synergy as a fixed group of muscles whose activity scales together, while observed electromyographic (EMG) patterns will generally consist of the combination of several such synergies and therefore need not show a fixed relationship in the relative amplitudes of their muscle activities.

Indeed in previous work, the examination of EMGs activated for rather constrained task conditions has generally not revealed fixed patterns. For instance, in an investigation of isometric precision grip, although some coupling of muscles was found, muscles that appeared correlated at one level of force magnitude were not necessarily so at a different level (Hepp-Reymond et al. 1996). It was concluded that muscles, although not controlled individually, can be grouped in a flexible fashion by the CNS to accomplish the same general task. In earlier work on postural control of stance in the intact cat, Macpherson (1988) had also concluded against fixed EMG patterns. A more recent study of stance perturbation in humans reached a similar conclusion, but did point out that recruitment of muscles appeared to cluster into groups, according to the direction of perturbation (Henry et al. 1998). Although these studies have hinted at the possibility of muscle groups, their methods of analysis (correlation of muscle activation levels, muscle tuning curves) were better suited for a search of fixed EMG patterns than for an evaluation of the hypothesis of fixed synergies embedded within EMG patterns (see DISCUSSION).

Address for reprint requests: E. Bizzi, Massachusetts Institute of Technology, Dept. of Brain and Cognitive Sciences, 77 Massachusetts Ave., E25-526, Cambridge, MA 02139 (E-mail: emilio@ai.mit.edu).

The costs of publication of this article were defrayed in part by the payment of page charges. The article must therefore be hereby marked "*advertisement*" in accordance with 18 U.S.C. Section 1734 solely to indicate this fact.

Better evidence for the control of groups of muscles was obtained in another stance perturbation study where muscle activation levels were correlated to nonmuscle (force/torque) parameters (Jacobs and Macpherson 1996).

The above studies were centered on a particular task (for example, postural control with the production of an invariant force direction at the ground for a range of perturbation directions). However, to critically test for fixed synergies embedded within EMG patterns, it would appear preferable to include a large range of tasks. The idea is that if a key aspect of motor control consists of combining a limited set of fixed synergies, one should be able to extract these synergies as building blocks whose combinations would explain the EMG patterns observed in a wide variety of different tasks. The importance of combinations in motor control has already been suggested theoretically by other investigators (Berkinblit et al. 1986; Grillner 1981). In a recent computer simulation exploring pedaling tasks with a variety of biomechanical requirements, it was found that this range of tasks could be executed well with muscles controlled as groups (Raasch and Zajac 1999). In addition, some investigators have interpreted their EMG results as evidence for shared circuitry in different tasks. For example, in the turtle, the rostral scratch and forward swimming share several features such as knee extensor activity during the latter half of hip flexor activity (Field and Stein 1997), which is the key distinction from other forms of scratch. In the cat, there is EMG evidence that circuitry is shared between scratching and locomotion (Deliagina et al. 1981), or between different forms of locomotion (Buford and Smith 1990; but see Grasso et al. 1998).

The concept of synergy would be most useful, if it could be arrived at in a complementary way that, rather than relying on a comparison of multiple tasks or behaviors, was instead task-independent, and based on neural organization. It is known that the spinal cord, disconnected from the brain, can generate fairly complex muscle activation patterns that resemble those seen in natural behaviors (Pearson and Rossignol 1991). This suggests that muscle synergies could already be assembled at the level of the spinal cord. In fact a recent analysis using a computational algorithm has shown that the spinal cord motor output could be reconstructed as the flexible combination of muscle synergies, but this experiment was limited to withdrawal from cutaneous stimulation of the hindlimb (Tresch et al. 1999). A recent study of hindlimb wipes in the spinal frog has also provided evidence for the control of muscle groups (Kargo and Giszter 2000). Interneuronal circuitry would be expected to play a key role in the spinal assembly of muscle synergies. In the present study, we used the experimental paradigm whereby focal *N*-methyl-D-aspartate (NMDA) iontophoresis in interneuronal regions of the frog's spinal cord elicits at active sites an organized motor output that is rhythmic, or less often tonic. This output, when described in terms of the isometric forces recorded at the ipsilateral ankle, is discrete in the sense that the directions of all these forces are limited to a few orientations (Saltiel et al. 1998). The rhythms themselves fall in a few major classes according to the force directions entering in their composition. Although this perhaps suggests a link with natural tasks, we have the advantage with this method that we are stimulating focally a large number of regions of the spinal cord, with the output determined by the spinal cord organization rather than by specific externally imposed tasks. Thus any synergies that we find with this method may more genuinely reflect what is basically encoded within the spinal cord rather than be partly a reflection of the particular task being carried out. The latter situation has often complicated the interpretation of EMG patterns in natural movements. Another advantage of this task-independent method is the simpler spinal preparation with the hindlimb held isometrically, with fewer modulating inputs than in an intact freely moving frog, which would be required to include behaviors such as locomotion or swimming when searching for a set of synergies common across tasks. In addition, although beyond the scope of this paper, the NMDA microstimulation technique has the potential of providing topographic information about the circuits that would encode the spinal synergies.

Here we report on the extraction of a set of seven muscle synergies, similar between frogs, whose linear combinations can account on the average for more than 96% of the variance of the EMG patterns elicited by chemical stimulation of the spinal cord interneurons. We also present evidence that these synergies occur in preferred combinations to generate the EMG patterns.

METHODS

Surgery

This has been described in detail previously (Saltiel et al. 1998). All procedures were approved by the Animal Care Committee at MIT. Briefly, after anesthesia with 1 ml of Tricaine methanesulfonate subcutaneously supplemented by ice, the frog (*Rana catesbeiana*) was spinalized at the level of the obex. The lumbar spinal cord was exposed by laminectomy. The dura was opened with electrocautery, and the pia with fine scissors. Twelve muscles of the hindlimb were implanted with bipolar EMG electrodes (see Fig. 1, legend). Most of these muscles are biarticular. However, their actions have been characterized as force fields by electrically stimulating the individual muscles and recording the forces they produce at the ankle in different isometric limb configurations (Loeb et al. 2000). Accordingly, the rectus internus (RI) and adductor magnus (AM) force fields are hip extensor and knee flexor; semimembranosus (SM) hip extensor; semitendinosus (ST) predominantly knee flexor; iliopsoas (IP) and rectus anterior (RA) hip flexor; vastus internus (VI), vastus externus (VE), and peroneus (PE) knee extensor; biceps femoris (BF) and sartorius (SA) hip flexor and knee flexor. Gastrocnemius (GA) is a knee flexor and plantarflexor.

Iontophoresis

A 2.5-μm tip three-barrel pipette was used. Besides the NMDA barrel, one barrel was for current balancing, and the third available for electrical stimulation. Another pipette was glued to the side for recording. NMDA was iontophoresed with parameters (-100 nA, for a maximum of 30 s or up to the time of onset of EMG activity), which should be associated with a spread of 150- to 270-μm radius by the average time of onset of EMG activity (Saltiel et al. 1998).

Data recording

The ipsilateral hindlimb was placed in a force sensor apparatus and held isometric in a standard position (hip and knee angles of 74 and 79°). EMGs and forces were recorded for 60 s starting with the onset of NMDA iontophoresis. In one frog (*F162*), they were recorded for two 60-s periods separated by a brief interruption. EMGs were amplified 25,000 times and sampled at 2,000 Hz, and the forces in three dimensions were simultaneously recorded. NMDA was generally

applied at depths of 500, 800, and 1,100 μm, 200–400 μm from the midline. Our previous study has shown the focality and the reproducibility of this method and provided evidence from simultaneously applied TTX that the effects of NMDA represent interneuronal stimulation.

Data analysis

The records with EMG activity were down-sampled to 1,000 Hz. The first second of the records was averaged and subtracted as the baseline to remove any possible tonic noise bias. The records were parsed as successive EMG responses, using interactive software from Matlab. Any visually significant change in the ongoing EMG activity from the 12 muscles was marked as a different response. In this way, we hoped to avoid forced grouping of muscles.

To assess whether this manual division of the EMG data introduced a bias in the results reported here, the same data were automatically parsed in 200-ms consecutive responses, from onset to offset of EMG activity in the record. Although bias-free, a possible disadvantage of automatic parsing is that if an EMG transition lies within the parsed interval, details may be lost when averaging EMGs in the next step. Another difference between manual and automatic parsing is that long stable EMG responses will be over-represented with automatic (divided in many), but counted as one with manual parsing.

Once the onsets and offsets of the responses were determined, the EMGs were rectified, and the first second of the records subtracted again to remove any oscillatory noise about zero that could have remained uncorrected after the first unrectified baseline subtraction. Each rectified EMG response was averaged between its time of onset and offset to a single value for each of the 12 muscles. In each frog, these EMG values were subsequently normalized for each muscle to the maximal EMG activity recorded in that muscle from any response from that frog. This was done to correct for possible "electrode sampling" differences between frogs.

Extracting algorithm

We quickly assessed the dimensionality of our observed EMG patterns with principal component analysis (PCA), using Matlab. PCA is a commonly used method to search for a small number of components whose combinations account for the observed data (Flanders 1991; Soechting and Lacquaniti 1989). However, a possible problem with using PCA for extracting synergies is that because the principal components are constructed as an orthogonal set, some of the muscle activations comprising a synergy might turn out to be negative. Instead we extracted the synergies by using a modified version of our previously described iterative algorithm (Tresch et al. 1999). Starting with a specified number of random initial synergies, a nonnegative least-squares method (Lawson and Hanson 1974) was used to find for each observed EMG response the coefficient of activation of each synergy so that their linear combination best approximated the EMG response. This procedure, supplied in Matlab (nnls), is analogous to standard regression techniques except that the weighting coefficients are constrained to be positive. In the next step of the iteration, we did not use gradient descent as in the original extracting algorithm to update the synergies. Rather, we used again nnls to construct a new set of synergies one muscle at a time, such that multiplied by the set of coefficients of activation obtained in the previous step, the linear combination of these synergies best accounted for the set of EMG responses. This process of alternating least squares was iterated 1,000 times. After each iteration, the R^2, i.e., the amount of variance of the EMG data explained by the updated set of synergies and their coefficients, was determined. After the last iteration, the synergies were normalized for comparison with other frogs by making the vector norm of each synergy equal to one.

As indicated previously (Tresch et al. 1999), the algorithm generally requires around 50–100 responses to produce consistent results. Because the average number of responses elicited by NMDA at active sites was 41 $\pm$ 48, the algorithm was not applied to the data from individual sites. The algorithm was run five times each to extract 4, 5, 6, 7, or 8 synergies from each individual frog's entire EMG data set, as well as from the pooled responses from all 10 frogs. Because the algorithm started from random initial synergies, it sometimes found more than one solution, i.e., two (28%), rarely three (6%) on different runs on the same data set. The algorithm was robust in that increasing the number of runs beyond five did not increase the number of solutions. In particular, in two data sets (1 from *frog F145* and another the pooled data), where three different solutions had been found in five runs of the algorithm, no additional solution was found after increasing the number of runs to 29–37. Importantly, when the algorithm found alternative solutions in the extraction of a given number of synergies from a data set, they were both implemented when extracting an additional synergy from the same data. This was observed in 14/15 cases in 10 frogs. An example will be illustrated in Fig. 4 (see RESULTS).

Reconstruction of the EMG data

To reconstruct a response, the extracted synergies were added after multiplying them by their coefficients of activation for that response. The reconstructed response was compared with the observed response by computing the normalized dot product between the two, a value of 1 indicating a perfect reconstruction.

Comparison of synergies extracted in different frogs

This was done both to assess the similarity between frogs, and to help in choosing the single best solution of the extracting algorithm applied to the pooled data from the 10 frogs. The best-match procedure between two sets of synergies of equal size involved computing the normalized dot product between all possible pairs of synergies from the two sets. The pairing providing the best overall match was selected. Because seven synergies were needed to account for more than 90% of the variance in the pooled data, we focused our comparison on sets of seven and eight synergies. We selected for each frog its seven-synergy solution that best matched a given seven-synergy solution from the pooled data. This permitted to align 10 sets of 7 synergies, according to their match with the 7 synergies from the pooled data. The similarity of synergies across the 10 frogs was then determined by averaging for each synergy its 10 normalized dot products with the corresponding synergy from the pooled data. This procedure was repeated for each of the three seven-synergy solutions and for the single eight-synergy solution from the pooled data. We chose as the best seven-synergy solution from the pooled data the set whose individual synergies matched most consistently across frogs (see RESULTS).

We also used a slightly different method to find the single best 7-synergy solution for the 10 frogs. Here we took the results of the five runs of 7-synergy extraction from each frog and used the *k*-means clustering algorithm to group these 350 synergies into 7 distinct categories (Hartigan and Wong 1979). This analysis gives an equal weight to each frog. The *k*-means algorithm starts with a specified number of cluster centers. It then assigns each data point (here extracted synergy) to the cluster with which center it has minimal distance (computed as 1 minus the normalized dot product). In the next step, it recalculates the centers by averaging the members of its cluster. This process is repeated until the mean of the distances between the elements of the clusters and their centers decreases by $<$0.1%. We applied the *k*-means procedure 400 times, each time starting with 7 random initial synergies as centers, which produced some variability in the clustering. Of the 400 trials, we determined the one solution with the tightest clusters (highest grand mean of the mean normalized dot product for each cluster of its synergies with its center). It was compared with the results of *k*-means initialized with

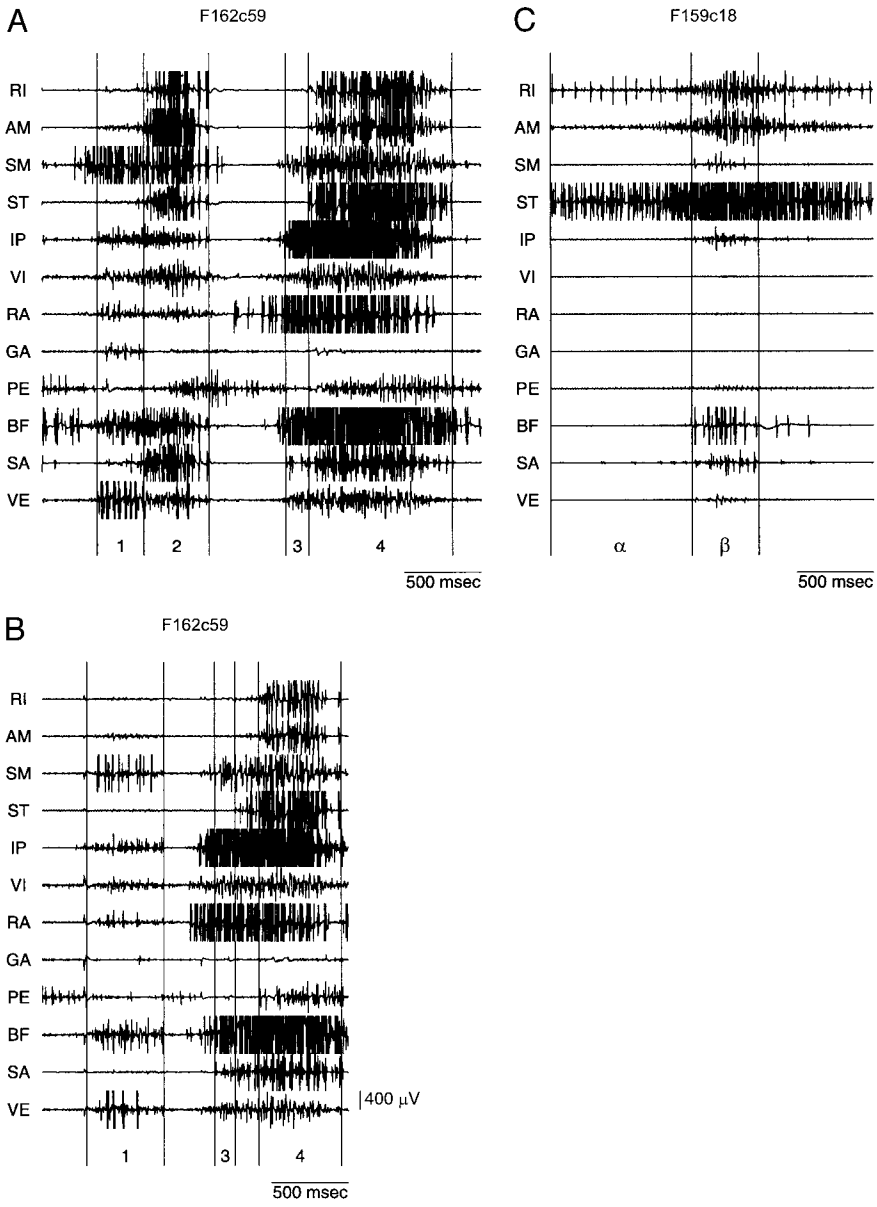

FIG. 1. Examples of electromyographic (EMG) sequences: evidence for embedded synergies from visual inspection. *A* and *B*: 2 sequences from a single *N*-methyl-D-aspartate (NMDA) application to a spinal cord site in one frog (*F162*). Weak EMGs began 11 s after the onset of NMDA iontophoresis, which was applied for a total of 30 s. The sequences shown in *A* and *B* are later in time, i.e., approximately 62 and 67 s after the end of this application, and are representative cycles of the rhythm obtained from this site. The recorded muscles were as follows: RI, rectus internus; AM, adductor magnus; SM, semimembranosus; ST, semitendinosus; IP, iliopsoas; VI, vastus internus, RA; rectus anterior; GA, gastrocnemius; PE, peroneus; BF, biceps femoris; SA, sartorius; VE, vastus externus. Responses representing important phases in the cycle are divided by vertical lines and labeled (*phases 1–4*). The detailed manual parsing of the EMGs for the sequence in *A* is shown in Fig. 3. *C*: sequence from another frog (*F159*). EMGs began 27 s after the onset of NMDA iontophoresis, which was stopped 1 s later. The illustrated sequence begins 14 s after the end of this application. Two phases are labeled (α, β). Amplitude scale same for all EMGs of Fig. 1.

the three different seven-synergy solutions of the extracting algorithm for the pooled data.

The final result was a single best 7-synergy solution for the 10 frogs. We labeled these synergies A to G. For the subsequent analysis of combinations, the set of seven synergies chosen for each individual frog (when there was more than 1 solution of the algorithm) was the one with the highest overall match to the A–G seven-synergy solution for the pooled data.

Exploring preferred combinations of synergies

We reasoned that if there were preferred combinations, they should appear when the extracting algorithm was used to account for the same data from each frog with a set of synergies smaller than seven (i.e., 4, 5, or 6). Using nnls, the best fit for explaining each synergy from these smaller sets as a linear combination of the synergies from the set of seven from the same frog was computed. The quality of this fit was evaluated by computing the normalized dot product. To determine the frequency of occurrence of these combinations, their description was simplified by deciding that for a synergy from the set of seven to be considered part of a combination, its coefficient of activation had to be above a threshold of 0.1. The frequency of occurrence of each possible combination was determined in each frog. When pooling the frogs together, we labeled each frog's set of seven synergies as A to G according to its best overall match with the A to G synergies from the pooled data. In one frog, this match was reordered for a pair of synergies because it agreed better with visual inspection. In the few cases where a synergy from a frog poorly resembled the lettered synergy to which it was paired as a result of the match (normalized dot product <0.55), we did not keep this label. Instead we labeled the atypical nonmatching synergy with a different symbol in the description of the combination in which it entered (this happened for a single synergy in 4 frogs, i.e., 4 of the 70 synergies). In two of these frogs, another synergy was better described as a combination (D + G in one, and E + B in the other).

RESULTS

This report is based on the 109/455 (24%) of tested sites in the lumbar spinal cord that responded to NMDA in 10 frogs (11 ± 6 responsive sites per frog), as described previously

(Saltiel et al. 1998). The EMG patterns elicited at these 109 sites were parsed in a total of 4,454 responses (see METHODS).

Synergies underlying EMG patterns: an example that illustrates the hypothesis

Two EMG sequences elicited as part of a prolonged response to NMDA iontophoresis are shown in Fig. 1, *A* and *B*. Several important features can be seen when focusing on the four phases labeled *1–4* in Fig. 1*A*. It is clear that in Fig. 1*B*, very similar phases (*1*, *3*, and *4*) are also present, but *phase 2* has dropped. It can also be seen that both *phases 2* and *4* essentially represent a continuation of the EMGs active in *phases 1* and *3* (SM, IP, VI, RA, BF, and VE), to which other muscles (RI, AM, ST, PE, and SA) get added. In Fig. 1*C* from another frog, the reverse sequence occurs. Although some of the muscles are weakly activated, we first see RI, AM, ST, PE, and SA in isolation (phase α), which precedes the temporary addition of SM, IP, VI, RA, BF, and VE (phase β). These temporal features strongly suggest that at least some observed EMG patterns (e.g., *phases 2* and *4* in Fig. 1*A*, phase β in Fig. 1*C*) represent the summation of smaller groups of muscles.

Another relevant observation is that the muscles active in *phases 1* and *3*, although rather similar (SM, IP, VI, RA, BF, and VE), are in a very different balance (SM, VE, and BF strongest in *phase 1*, IP, RA, and BF strongest in *phase 3*). The SM, IP, VI, RA, BF, and VE added in phase β of Fig. 1*C* has only BF strong, a different situation from both *phase 1* of Fig. 1, *A* and *B* (where SM and VE were also strong), and from *phase 3* of Fig. 1, *A* and *B* (where IP and RA were also strong). These comparisons suggest that even the muscle patterns in *phases 1* and *3* may be constituted from smaller groups of muscles. For example, *phases 1* and *3* could both represent the summation of three synergies, one with SM, VE, one with BF, and one with IP, RA, but with each activated to a different relative degree in the two phases. Note that a similar argument could be made for the muscles added in *phases 2* and *4*, which again are the same (RI, AM, ST, PE, and SA), but in a different balance (e.g., AM strongest in *phase 2*, ST strongest in *phase 4*).

These and similar observations from many other records of raw EMG data strongly suggested the existence of synergies embedded within the observed responses. To explore whether the EMG patterns observed at any particular time could represent the summation of such synergies, we used a modification of a computational algorithm described previously (Tresch et al. 1999). This analysis is aimed at extracting a specified number of synergies whose positive linear combinations best approximate the observed data (see METHODS).

Comparison between frogs to define an optimal set of synergies

When all frogs were pooled together, and the algorithm used to extract eight synergies, we found a very robust (single) solution that explained slightly more than 95% of the variance in the EMG data. This agreed well with the result of PCA on the same pooled EMG data: eight principal components were necessary to account for more than 95% of the variance in that data. The match across frogs (see METHODS) was generally very good for seven of the eight extracted synergies (0.977 ± 0.016, 0.783 ± 0.113, 0.954 ± 0.049, 0.905 ± 0.052, 0.927 ± 0.048, 0.897 ± 0.097, and 0.833 ± 0.102), but much poorer for one of the synergies (0.672 ± 0.265). This suggested that a set of seven synergies might be sufficient to account adequately for the data.

Linear combinations of seven synergies could explain more than 91% of the variance in the pooled data from all ten frogs. In individual frogs, a set of seven synergies (taking the highest R^2 solution, i.e., the one explaining the most variance when there was more than one solution 5/10 frogs) was able to account on the average for $96.49 \pm 1.07\%$ of the variance in the data. In contrast, for two random simulations of EMG data, only $63.23 \pm 0.40\%$ of the variance could be explained on extracting seven synergies from the random data.

The algorithm found three solutions for the extraction of seven synergies from the pooled ten frogs (R^2 of 0.9207, 0.9193, and 0.9156). No other solution appeared in a total of 37 runs of the algorithm on the same data. These solutions (Fig. 2, *A–C*) have many features in common, with two major differences. *1*) In Fig. 2*A*, synergy vi, RA, sa (weaker muscles in lowercase) is separate from synergy IP, vi, sa and from synergy VI, PE, but the former two are combined in Fig. 2*B*, and the latter two are combined in Fig. 2*C* (where there is also some redistribution of PE to the GA, pe synergy). *2*) In Fig. 2, *B* and *C*, synergy ri, ST is separate from synergy RI, AM, sm, SA and from synergy sm, ip, BF, but it is combined with both of them in Fig. 2*A*. A minor difference is the presence of some BF in the SM, VE synergy in Fig. 2*A*.

To evaluate which of these seven-synergy solutions might constitute the best solution, we assessed how each of these solutions matched across the individual frogs.

For the first solution of seven synergies from the pooled data (Fig. 2*A*), the match across frogs was distinctly poor for the IP, vi, sa synergy (0.617 ± 0.300), while the other six synergies matched well (0.972 ± 0.017, 0.856 ± 0.138, 0.805 ± 0.108, 0.855 ± 0.080, 0.872 ± 0.238, and 0.798 ± 0.127). In the case of the second solution of seven synergies from the pooled data (Fig. 2*B*), we found a good to very good match across frogs for all seven synergies without exception (0.902 ± 0.159, 0.771 ± 0.203, 0.915 ± 0.038, 0.846 ± 0.098, 0.908 ± 0.050, 0.770 ± 0.127, and 0.772 ± 0.189). For the third solution of seven synergies (Fig. 2*C*), there was again a less good match across frogs for two of the synergies (0.910 ± 0.113, 0.720 ± 0.264, 0.955 ± 0.031, 0.901 ± 0.063, 0.929 ± 0.045, 0.871 ± 0.172, and 0.682 ± 0.183).

The second solution (Fig. 2*B*) also agreed better with our impressions based on visual inspection of the data.

Further support for the second solution came from a *k*-means clustering analysis performed on the synergies extracted from the individual frogs. Out of 400 randomly initialized *k*-means analyses on these synergies, we sought the one solution with the tightest clusters (see METHODS). It occurred on five occasions, with an overall match for each cluster of its synergies with its center of 0.897 ± 0.065. The centers of these clusters, shown in Fig. 2*D*, defined a set of seven synergies quite comparable to the second seven-synergy solution extracted from the pooled data (Fig. 2*B*), with a match between these two sets of 0.950 ± 0.015. In addition, when *k*-means was initialized with the three different seven-synergy solutions extracted from the pooled data, the initialization with the second solution gave an identical result to the tightest clusters found with the randomly initialized *k*-means procedure.

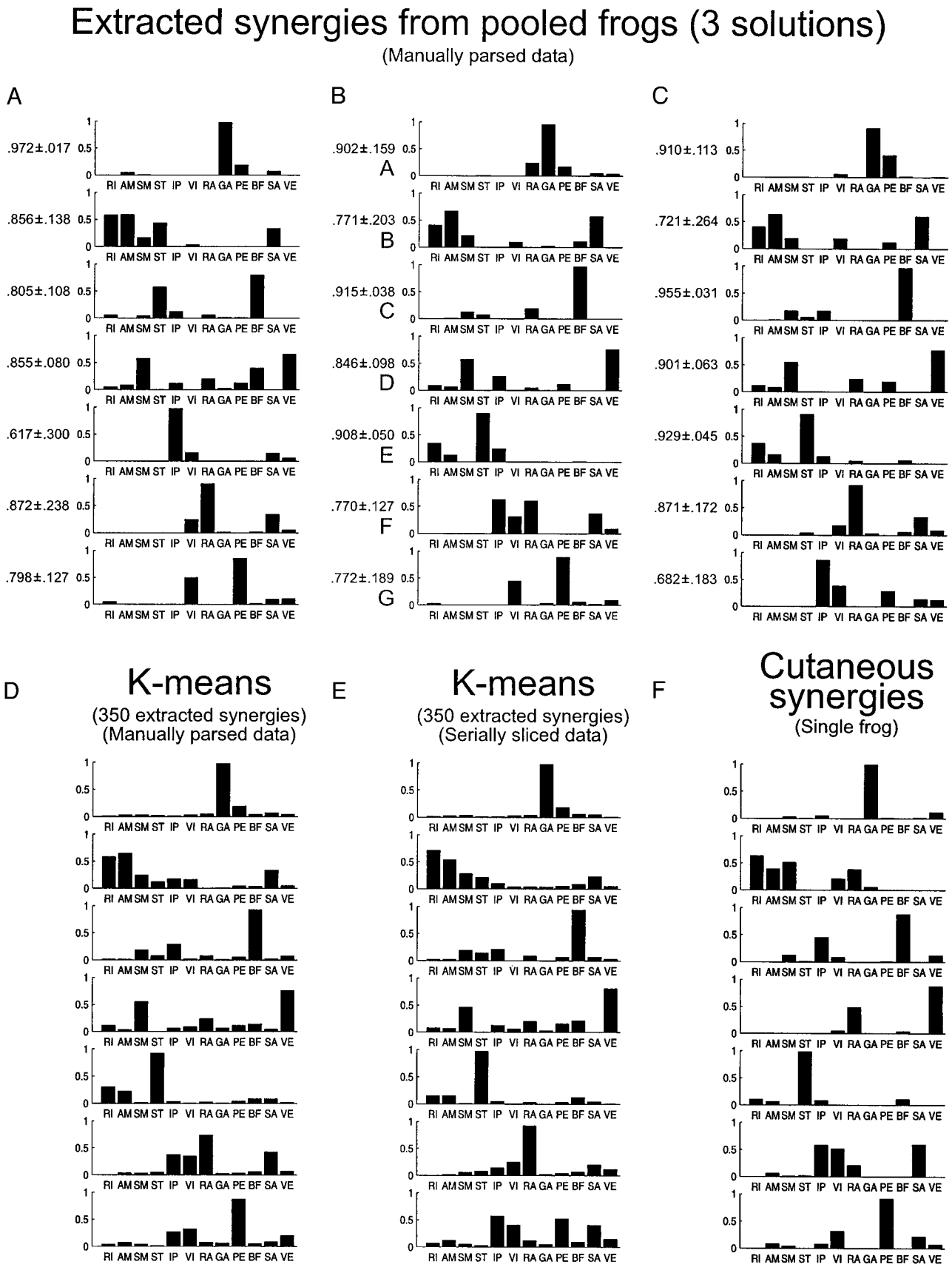
Extracted synergies from pooled frogs (3 solutions)
(Manually parsed data)
A
B
C
.972±.017
.856±.138
.805±.108
.855±.080
.617±.300
.872±.238
.798±.127
.902±.159
.771±.203
.915±.038
.846±.098
.908±.050
.770±.127
.772±.189
.910±.113
.721±.264
.955±.031
.901±.063
.929±.045
.871±.172
.682±.183
RI AM SM ST IP VI RA GA PE BF SA VE
D
K-means
(350 extracted synergies)
(Manually parsed data)
E
K-means
(350 extracted synergies)
(Serially sliced data)
F
Cutaneous synergies
(Single frog)

We therefore adopted this solution for the continuation of the analysis in this paper. The synergies of Fig. 2*B* were labeled A to G in the order shown.

As a validation of our parsing of the data set, we also applied the synergy extraction algorithm on the EMGs divided into equal time intervals rather than the manual identification of onsets and offsets used above (see METHODS). For the synergies extracted in this fashion, the *k*-means solution with the tightest clusters, shown in Fig. 2*E*, is quite similar to the solution of Fig. 2*B*, with an overall match of 0.954 ± 0.056. The similarity is particularly striking for synergies A to E, while some difference can be appreciated for synergies F and G, which actually look closer to the solution of Fig. 2*C*.

In conclusion, we have identified a set of seven synergies, similar between frogs (Fig. 2*B*), and whose linear combinations account for more than 91% of the variance in the pooled data. While the similarity between the results of *k*-means applied to the manually and automatically parsed data are strongly reassuring, it also indicates that some degree of uncertainty persists about the precise balance of muscles active in synergies F and G.

For comparison with the NMDA synergies, we extracted seven synergies from the EMG patterns of a range of cutaneous behaviors that included rostral wipes, caudal wipes, and withdrawals in two frogs, and rostral wipes and withdrawals in a third frog. Figure 2*F* illustrates the result in one frog (*F144*). Although some differences are seen between the synergies of Fig. 2*B* (NMDA) and of Fig. 2*F* (cutaneous), in particular for the distribution of SM, they were overall rather similar with a match of 0.847 ± 0.120. Cutaneous synergies extracted from a second frog (*F162*) did not match as well the NMDA synergies of Fig. 2*B* (0.740 ± 0.240); however, that same frog had one unusual NMDA synergy (illustrated in Fig. 3*C*). The match between the cutaneous and NMDA synergies within that frog was good at 0.833 ± 0.206, again with a different distribution of SM in the cutaneous versus NMDA synergies. For a 3rd frog with only 11 muscles recorded (no PE), comparison of its cutaneous synergies with the NMDA synergies extracted from the pooled 10 frogs after leaving out PE from their EMG responses again showed a good match at 0.847 ± 0.118. Overall, these results of similarity of the NMDA to the cutaneous synergies support the physiological relevance of our NMDA synergies (see DISCUSSION).

We also extracted five cutaneous synergies from the same three frogs, after removing the three muscles (RA, GA, and PE) that were not recorded in the study of limb withdrawals (Tresch et al. 1999). Four of the synergies were quite comparable to those previously reported, and there was an additional fifth synergy that corresponded to the inclusion of caudal wipes in our cutaneous behaviors.

Example of EMG pattern reconstruction

Figure 3*A* shows the EMG data of Fig. 1*A*, after rectification, averaging, and normalization of the EMGs (see METHODS). Its reconstruction with seven synergies extracted from the entire data set of that frog (*F162*) is shown in Fig. 3*B*. There was generally an excellent agreement between the observed and reconstructed data. For these 15 responses, the average normalized dot product was 0.970 ± 0.040. The synergies identified by the algorithm are shown in Fig. 3*C*. Six of the seven synergies were similar to those extracted from the pooled frogs (labeled B–G, compare with Fig. 2*B*), while the first synergy was unusual. For each synergy, the coefficients of activation for *phases 1–4* are also shown. Note that the BF (*C*) and SM, VE (*D*) synergies are co-activated with an opposite predominance in *phases 1* and *3;* and that the RI, AM, SA (*B*) and the RI, ST (*E*) synergies are not active until *phases 2* and *4* when they are both added, again with an opposite predominance. Thus, in this example, different phases of the rhythm shared pairs of synergies in their construction, but with opposite balances of activation within each pair.

Exploration of synergy combinations

The extracted synergies can be considered as building blocks that combine linearly to produce the EMG patterns underlying the forces elicited by focal NMDA iontophoresis. Since a limited number of force orientations occurs (see INTRODUCTION), one might expect that the synergies do not combine in any possible way, but that there are preferred combinations.

We reasoned that if there were preferred combinations of synergies, they should appear when the extracting algorithm was used to account for the same data from each frog with a set of synergies smaller than seven (i.e., 4, 5, or 6). This is because the algorithm in each case is designed to account for the maximum amount of variance in the data.

Thus to find the combinations, we extracted sets of four, five, or six synergies from each frog. Each synergy from these smaller sets was then fitted as a linear combination from the set of seven synergies extracted from the same frog (see METHODS). For the 10 frogs, this fitting was possible with a mean normalized dot product of 0.992 ± 0.004 ($n = 750$). An example is shown in Fig. 4. In this frog (*F145*), of three solutions for seven synergies, the one explaining the most variance (Fig. 4*A*) matched best the solution from the pooled data (compare with Fig. 2*B*), and its synergies were labeled A to G by correspondence to that solution. For six synergies, there were three solutions and for five synergies a single one. Compared to the seven-synergy solution, the six-synergy solution of Fig. 4*B* differed chiefly through the combinations of B + E and of C + E, while instead the six-synergy solution of Fig. 4*C* differed through the D + G combination. In Fig. 4*D*, the single five-synergy solution differed chiefly from the seven-synergy solu-

FIG. 2. Synergies: extractions from the pooled NMDA data. *A–C*: the 3 solutions for 7 synergies ($R^2 = 0.9207$, 0.9193, and 0.9156, respectively) extracted from the pooled EMG responses from all 10 frogs ($n = 4{,}454$ responses). For each synergy, the average match across individual frogs is indicated (mean ± SD). The solution shown in *B* was chosen as the best solution (see text). Its synergies are labeled A to G. *D*: the centers of the 7 tightest clusters found out of 400 runs of randomly initialized *k*-means applied to the 50 sets of 7 synergies extracted from 10 frogs. *E*: the same *k*-means analysis applied to the synergies extracted from the serially sliced instead of manually parsed data. *F*: the cutaneous synergies extracted from one frog. These were extracted from serially sliced data ($n = 1{,}729$ responses). There was another solution than the one illustrated, which looked closer to Fig. 2*C* (match 0.861 ± 0.100).

tion through the combinations B + E, C + E, and D + G, i.e., the different combinations seen above. Figure 4*E* quantitatively shows these five synergies fitted as A + D, B + E, C + E, D + G, and C + F. The suggestion from this analysis would be that these five synergy combinations are important in the reconstruction of this frog's EMG data.

This suggestion of preferred combinations of synergies is supported by a different analysis where we computed pair-wise

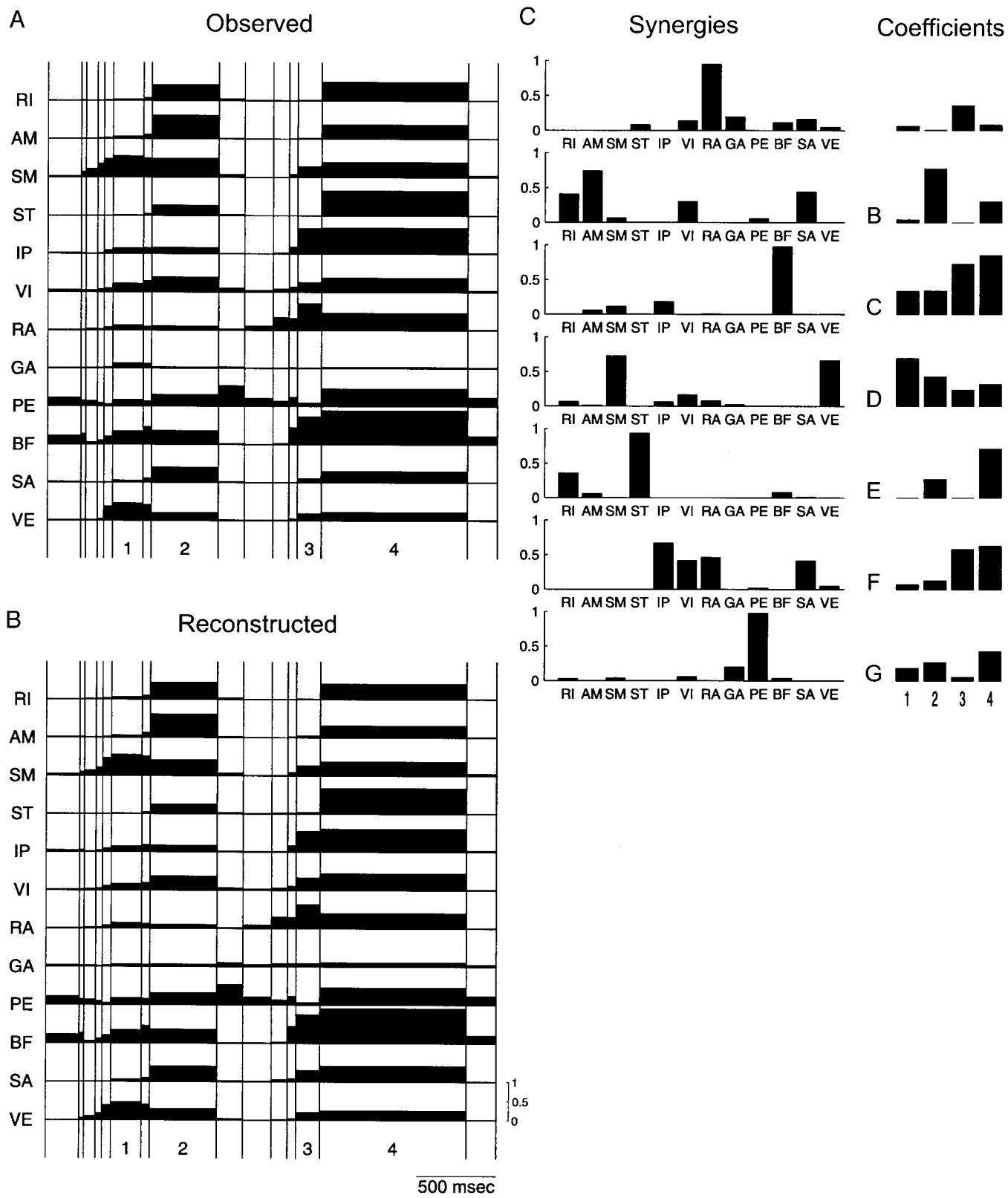

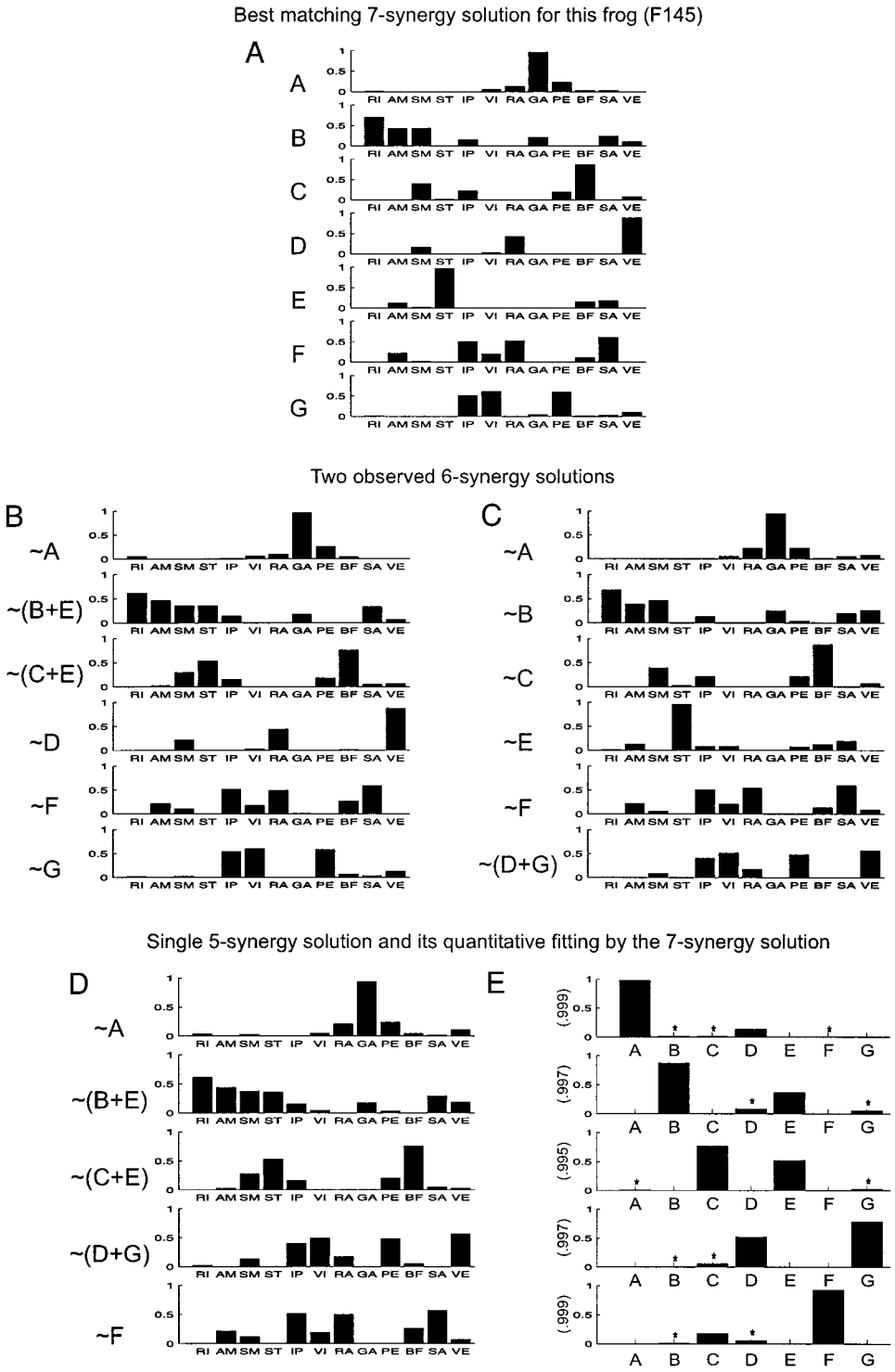

FIG. 4. Method for the identification of synergy combinations: illustration from an example. *A*: the 7-synergy solution from this individual frog (*F145*) that best matched the solution from the pooled data (Fig. 2*B*). Its synergies are labeled A to G. *B–D*: 2 of 3 observed solutions for 6 synergies, and the single solution for 5 synergies in this same frog described as combinations from those shown in *A*, on the basis of visual inspection. *E*: an example of quantification of these combinations. The heights of the A–G bars indicate here the combinations of the 7 synergies of *A* that provided the best fit to the individual synergies of *D*. Asterisks indicate synergies that contributed little to a combination (coefficients of activation between 0 and 0.1). These are, however, included in the computation of the normalized dot product on the ordinate that indicates the quality of the fit provided by each combination. The 3rd solution for 6 synergies and the solutions for 4 synergies, although not shown, were included in a similar fashion in the analysis of the combinations for this frog.

FIG. 3. EMG sequence reconstructed with 7 extracted synergies and their coefficients of activation. *A*: the EMG sequence of Fig. 1*A* rectified, averaged, and normalized for each muscle to its maximum activity observed in that frog. Vertical lines indicate how the sequence was actually parsed (e.g., note that *phase 1* is a bit different from that in Fig. 1). *B*: the same EMG sequence reconstructed. *C*: the 7 synergies utilized in the reconstruction. These synergies were extracted from the entire set of responses (n = 1,044) in this frog, and their coefficients of activation were simultaneously determined by the algorithm for each individual response. These coefficients are illustrated for the responses labeled *1* to *4*. The vertical scales apply both to the synergies and the coefficients. In this frog, the algorithm had actually found 2 different solutions when extracting seven synergies: they accounted for 0.9494 and 0.9492 of the variance in the data. Because the latter solution matched best the one for the pooled data from all frogs (compare with Fig. 2*B*), it was the one chosen for this reconstruction. B to G refer to synergy labels by correspondence to Fig. 2*B* (see METHODS).

the 21 correlation coefficients between the levels of activation of synergies A to G as they reconstructed this frog's EMG data. The five highest correlations were for the AD, BE, CE, DG, and CF pairs, which are the same combinations as those identified by the method described above in the analysis of this frog's single solution for five synergies (Fig. 4*E*). To systematically validate this method of identifying synergy combinations, we determined for each frog the four combinations of seven synergies that provided the best fit to its solution for four synergies. We then examined for the synergy pairs contained within these combinations how the correlation coefficients between their activation levels in the reconstruction of the EMG data ranked among the 21 theoretically possible pairs. By pooling all frogs, we obtained a histogram of the distribution of these ranks. This is shown in Fig. 5. It is clear that the majority of pairs present in the synergy combinations identified by our method correspond to the pairs of synergies with the highest correlation coefficients in the reconstruction of the EMG data.

A representative example illustrating further the correspondence between the identified synergy combinations and the EMG data are shown in Figs. 6 and 7. In this frog (*F149*), the solution for four synergies with the highest R^2 (0.9220) corresponded to the combinations A + D, B + E, C + D + G, and F + G (Fig. 6*A*) of the single seven-synergy solution for this frog. The correlation coefficients for the corresponding AD, BE, CD, CG, DG, and FG pairs present within these synergy combinations had again generally high ranks (6, 4, 1, 3, 2, and 9, respectively) among the 21 possible pairs. To evaluate these combinations against the EMG data, the activation levels of their component synergies were plotted against each other for the entire set of EMG responses from this frog. In Fig. 6*B*, we see that, although our identified F + G combination only ranked 9 by the correlation measure, it clearly accounts for an important feature of the data, namely that F and G are highly correlated (closely co-vary) for a subset of responses (labeled +). In the CD, CG, and DG plots, we also see a large subset of responses (labeled △), for which synergies C and D, C and G, and D and G are correlated. This subset of responses is distinct from the one for which F and G are correlated (compare nonoverlapping distributions of + and △). The BE plot also shows correlation between synergies B and E. These results therefore suggest that the identified F + G, C + D + G, and B + E combinations are indeed key in reconstructing the EMG data from this frog. The AD plot is different, as it shows co-expression, but not co-variation, of synergies A and D for many responses. The identification of an A + D combination perhaps related to the fact that when the EMG data were reconstructed with the four combinations, a sizable number of responses were reconstructed with the A + D combination only, with none of the other three combinations contributing significantly. Such a situation did not occur for the other three combinations.

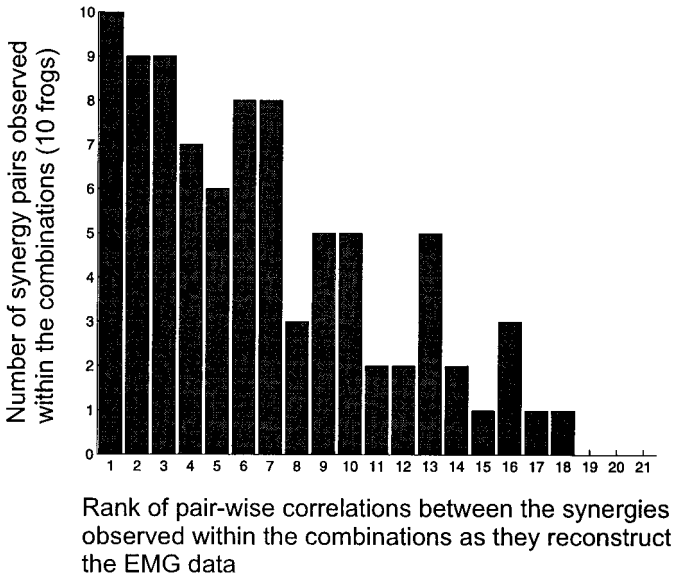

FIG. 5. Distribution of rank of the pair-wise correlations for the synergies observed within the combinations. For this validation analysis, only the extracted sets of 4 synergies (1 per frog; if there was more than a single solution for 4 synergies, 3/10 frogs, we chose the one explaining the most variance) were fitted as combinations of 7 synergies from the same frog. The average total number of synergy pairs within the 4 identified combinations was 8.7 ± 2.4 (n = 10 frogs; rarely a synergy pair occurred more than once within these combinations in a frog, but it was counted only once). For these synergy pairs, the rank of the correlations between their levels of activation as they reconstructed the EMG data were determined among the 21 theoretically possible pairs.

Further evidence for the identified synergy combinations being meaningful comes from examining their recruitment in a representative short EMG sequence from this frog (Fig. 7). An initial increase in A + D activity persists, followed by successive phases where the C + D + G, B + E, and F + G combinations become strongly active, with some degree of overlap. By comparing with the parsed EMG activity, it can be seen that together, these four combinations effectively delimit essential phases in the sequence.

We therefore adopted this method of expressing the synergies from the smaller sets as combinations from the set of seven, to identify the synergy combinations in each frog. We then pooled the 10 frogs together to examine the frequency of occurrence of these combinations, and in particular whether there are preferred combinations. The results are presented in Table 1. The number of frogs in which these different combinations were observed is also indicated. One hundred fifty-seven of 750 (20.9%) of the synergies from the smaller sets could be approximated as a single synergy from the set of 7, and 593 were combinations. The most frequent combinations were pairs (364 pairs/593 combinations = 61.4%). Three hundred thirty-two of these pairs were combinations of synergies labeled *A* to *G*, while the other 32 included an atypical synergy (see METHODS). Of 21 possible pairs of synergies A to G, 6 were distinctly common by their frequency of occurrence and because they occurred in at least three frogs (range 3–8, on the average 5 frogs). These pairs were A + D (29), B + E (57), C + D (41), C + E (49), D + G (14), and F + G (26). In addition, there were 25 instances of C + F in two frogs. Seven pairs were distinctly uncommon: A + C (0), A + F (0), B + C (0), B + G (0), D + E (0), D + F (0), and E + G (3, from 2 frogs).

Triplets accounted for 182/593 combinations (30.7%). Of 35 possible triplets of synergies A to G, 16 were not observed, and 8 occurred with a frequency <5. There were five common triplets: A + C + D (17), B + C + E (22), B + D + E (20), C + D + G (23), D + F + G (13), seen each in three to five frogs.

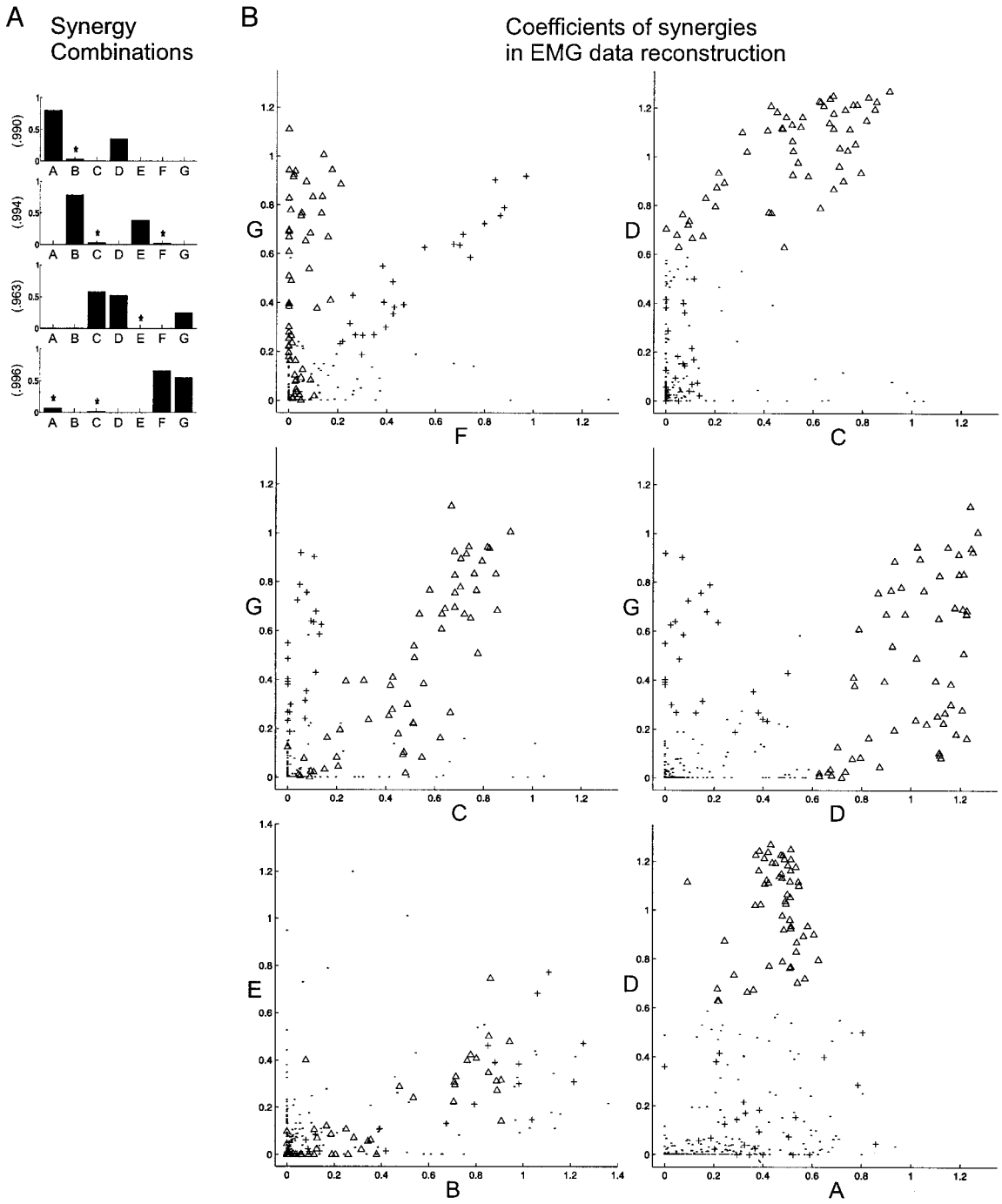

FIG. 6. Identified synergy combinations compared with coefficients of synergy activation in EMG data reconstruction. *A*: the set of 4 synergies explaining the most variance in this frog (*F149*) fitted as combinations of the 7 synergies extracted from this same frog (the A to G synergies are shown in Fig. 8*C*). Conventions are the same as in Fig. 4*E*. *B*: the coefficients of activation of the synergies plotted against each other as they reconstruct the EMG responses from this frog ($n = 361$). The pairs of synergies chosen are those within the combinations in *A*. +, the subset of responses for which F and G are correlated and F $\geq$ 0.2 (see FG plot, $n = 25$). △, the subset of responses for which C and D are correlated and D $\geq$ 0.6 (see CD plot, $n = 57$). ·, the remainder of the responses ($n = 279$).

DISCUSSION

Our study reports two main findings: *1*) the EMG patterns elicited by focal NMDA iontophoresis in the interneuronal regions of the spinal cord can be reconstructed as the linear combination of a small number of muscle synergies, and *2*) there are preferred combinations of these synergies.

The iontophoresis of NMDA was carried out in many different regions of the lumbar cord to obtain a good sampling across frogs. Previous work has established the focal nature of this method and also showed that the spinal cord output elicited by NMDA iontophoresis was abolished by focal TTX application at the same site. This was interpreted as strong evidence that the focal activation of interneurons is the essential neural substrate for the effect of NMDA (Saltiel et al. 1998). This does not exclude the

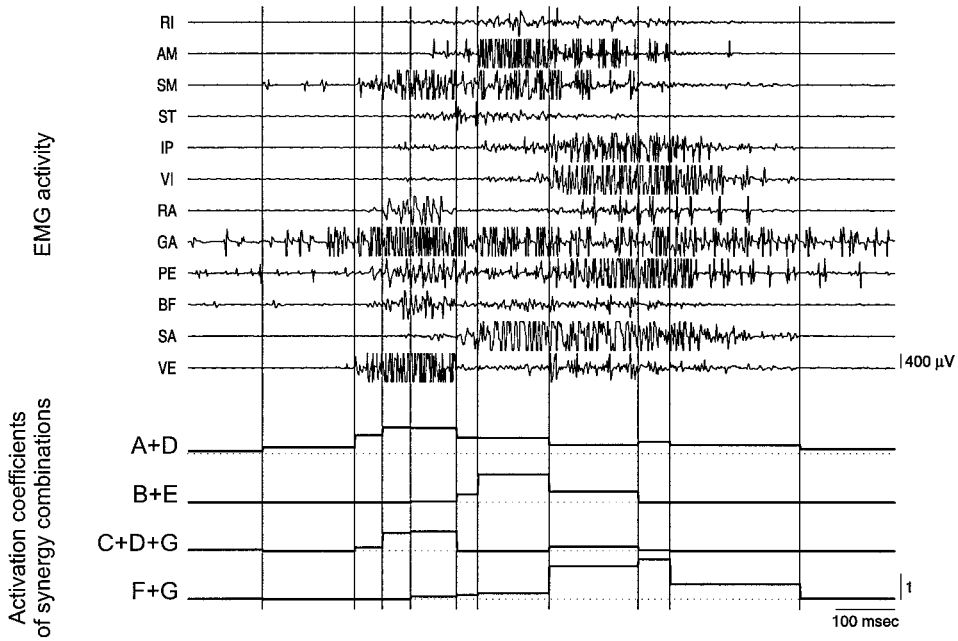

FIG. 7. EMG sequence reconstructed with synergy combinations. This EMG sequence is from the same frog as Fig. 6. The synergy combinations are those shown in Fig. 6*A*. Dotted lines indicate the zero activation levels of the synergy combinations. Vertical lines show the manual parsing of the EMG activity. For these 11 EMG responses, the average normalized dot product between the observed EMG activity, and the one reconstructed with these 4 synergy combinations was 0.949 ± 0.068. Amplitude scales the same for all EMGs, and the same for all coefficients.

possibility that the simultaneous focal activation of motoneuron dendrites might have some influence on the output elicited by NMDA. Recent reports of presynaptic NMDA autoreceptors on terminals in the spinal cord (Cochilla and Alford 1999; Liu et al. 1994) also raise the possibility of a modulatory influence at that level. However, it should be realized that, although our recorded EMG sequences are triggered by focal interneuronal stimulation, it is probable that they generally reflect the engagement of an extensive network through connectivity (Giszter et al. 1993; Saltiel et al. 1998). Therefore at that stage any additional focal modulatory influence on the motoneuron dendrites or nerve terminals locally present at the NMDA-responsive site might not have profound effects. Regardless of possible noninterneuronal contributions to the NMDA effect, three features support the physiological relevance of the NMDA-elicited EMG patterns. First, the motor output, described in terms of forces, is not random but organized in that it is characterized by clusters of force directions and preferred classes of rhythms (see INTRODUCTION). Second, the EMG output is organized since more than 90% of its variance is explained by the extraction of seven synergies compared with 63% of the variance of randomly simulated EMG data being explained by seven synergies extracted from that random data. Third, the synergies extracted from the pooled NMDA data are similar to the synergies extracted from a broad range of cutaneous behaviors (compare Fig. 2, *B* and *F*). The most striking difference is the absence of SM with VE (and its greater amount with RI, AM), in the cutaneous synergies. The reason for this difference is unclear. It is reminiscent of the observation in the cat whereby two muscles (lateral and medial gastrocnemius) that are both excited by a proprioceptive input can be differentially affected by a cutaneous input (sural nerve) that excites only one of the two muscles (LaBella et al. 1989; Nichols 1994).

TABLE 1. *Synergy combinations*

Pair Combination		Triplet Combination	
Pair	*n*	Triplet	*n*
AB	13 (2)	ABD	3 (1)
AC	0*	ABE	4 (1)
AD	29 (4)†	ACD	17 (3)†
AE	15 (1)	ACF	2 (1)
AF	0*	ACG	9 (2)
AG	15 (2)	ADF	11 (2)
BC	0*	ADG	8 (3)
BD	7 (3)	AFG	2 (1)
BE	57 (7)	BCD	6 (1)
BF	14 (1)	BCE	22 (5)†
BG	0*	BDE	20 (4)†
CD	41 (5)†	BFG	1 (1)
CE	49 (6)†	CDE	2 (1)
CF	25 (2)†	CDG	23 (4)†
CG	13 (2)	CEF	7 (2)
DE	0*	CEG	2 (1)
DF	0*	CFG	1 (1)
DG	14 (3)†	DFG	13 (3)†
EF	11 (1)	EFG	5 (1)
EG	3 (2)*	15 possible triplets	
FG	26 (4)†	were not observed	

The number of times (*n*) each listed combination from the set of 7 synergies (A–G) represented the best fit to the synergies from the smaller sets is indicated. The number of frogs ($n = 10$) in which these combinations were seen is also shown in parentheses. * Rare combination. † Frequent combination.

In our study, the EMG patterns elicited by NMDA were recorded from 12 muscles. Therefore identifying seven synergies whose linear combinations account on the average for more than 96% of the variance in individual frogs represents a mechanism of dimensionality reduction in motor control of the hindlimb, at the neuronal organization level (see INTRODUCTION). It may be mentioned in this context that a smaller set of five synergies was already able to account for 92.42 ± 2.36% of the variance in the NMDA data in individual frogs (and slightly over 85% of the variance for the pooled frogs). This indicates that a more impressive reduction of variables (from 12 to 5) already did a rather good job at reconstructing the NMDA EMG patterns recorded from 12 muscles. This result is not surprising given the finding of preferred combinations of the seven synergies when reconstructing the EMG data (Table 1).

The dimensionality reduction would be particularly meaningful

if it was certain that the range of EMG patterns elicited by NMDA iontophoresis in many different regions of the lumbar cord was as rich as that obtained by studying many different natural behaviors. The observations that intraperitoneal or subcutaneous injections of *N*-methyl-DL-aspartate in the adult spinal frog could elicit rostral wipes, stepping, kicking and jumping, and in the spinal tadpole, swimming (McClellan and Farel 1985) certainly suggest that focal NMDA iontophoresis might potentially activate any of the spinal circuits sub-serving these different behaviors. The similarity of the NMDA synergies to the synergies extracted from a broad range of cutaneous behaviors (Fig. 2 and RESULTS) is in keeping with that notion.

The extracted synergies from the NMDA data were overall quite similar between frogs. There was an average match across individual frogs of 0.841 ± 0.064 with the synergies from the pooled data (Fig. 2*B*), which were also markedly similar to the centers of the tightest clusters found by *k*-means applied to the synergies extracted from the individual frogs (compare Fig. 2, *B* and *D*). By contrast to this degree of similarity of the synergies between frogs, the average match between pairs of the seven synergies illustrated in Fig. 2*B* was 0.123 ± 0.072, indicating that the synergies were close to orthogonal (mean angle of 83 ± 4°, range 75–89°).

These synergies represent muscle linkages that remain preserved and embedded within the EMG patterns associated with the range of movements produced by NMDA. The alternative hypothesis to this synergy concept would be that for each type of movement, some new muscle coordination is put forward with no particular shared feature across the different movements. It seems to us that the explanation of more than 91% of the variance of the EMG data by a single set of synergies, similar across frogs, makes this alternative hypothesis less likely. The individual frogs could differ somewhat in their cord sampling and in the movements produced, rendering the similarity of the synergies extracted from their EMG patterns more significant. Future more direct analysis of this point would involve partitioning the NMDA data in different subsets on the basis of the simultaneously recorded force, and determining the degree to which synergies extracted from these different subsets are shared.

More generally, there remains the concern as to whether the synergies that we have extracted might simply represent the outcome of a statistical fitting technique rather than synergies genuinely encoded by the spinal cord. Again the comparison of our synergies to those extracted from many natural behaviors should help address this question. In particular, finding substantial sharing of synergies extracted from different EMG data sets, for example NMDA, a broad range of cutaneous behaviors, and swimming, would support the idea that these synergies represent building blocks for the construction of movement by the spinal cord. The finding of similarity between the synergies extracted from two data sets: NMDA and cutaneous (Fig. 2 and RESULTS) is a first step in that direction.

The idea that movements may be constructed from building blocks is not new. Sherrington (1910) has suggested that the spinal cord reflexes were the elemental building blocks on which movement was constructed, and Grillner (1981) has proposed that the combined activity of "unit burst generators," each controlling individual muscle groups, could form the basis for central pattern generation. The common feature of these hypotheses is that subgroups of muscles would be linked together as muscle synergies, and that flexible combinations of these subgroups would underlie different phases of the movement. This could be considered a more precise definition of the concept of modularity of the spinal cord motor system that was initially formulated in terms of force fields (Bizzi et al. 1991; Mussa-Ivaldi et al. 1994).

However, in the motor control literature, the existence of synergies has been doubted. One may therefore ask how our method of identifying rather robustly a set of synergies that would explain a large range of spinal motor behaviors differs from others. Essentially, this difference has to do with the distinction between fixed muscle patterns and fixed muscle synergies embedded within muscle patterns that need not be fixed (see INTRODUCTION). Other methods have looked for fixed patterns (Hepp-Reymond et al. 1996; Macpherson 1988) and failed to find evidence for them, whereas we have looked for evidence of fixed synergies embedded within EMG patterns, with positive results.

For example, a common approach has been to consider two muscles as part of a same synergy when their recruitment changes in parallel during variations of a task, e.g., when they have similar tuning curves of their activity against the direction of postural perturbation (Henry et al. 1998; Macpherson 1988). A potential problem with this approach can be seen when inspecting the synergy set of Fig. 2*B*. Here we have RA, SA together in synergy F. However, SA is also found without RA in synergy B. If synergies B and F were recruited in different contexts, e.g., in producing forces of different directions, then we might expect different tuning curves for RA and SA, and the false conclusion could be reached that no synergy with RA, SA exists.

Even when considering a single isometric force task, our approach may still give different results from other methods of identifying synergies. This possibility is shown in Fig. 8, whose data came from a single spinal cord site where the effect of NMDA essentially consisted of rhythmic caudal extensions. The parsed responses were divided into three groups of EMG magnitude (·, □, and * from weakest to strongest) by analogy with the analysis of hand synergies published by Hepp-Reymond et al. (1996), where subjects performed a precision grip isometric task at three levels of force magnitude. Applying this study's criteria, two muscles are considered to define a synergy when they are significantly correlated for at least two levels of magnitude. Accordingly, there would be evidence for a synergy with RI and ST (Fig. 8*A*, $R\cdot$ 0.56, $R\square$ 0.84, R^* 0.86), but not for a synergy with SM and VE (Fig. 8*B*, $R\cdot$ 0.31, $R\square$ 0.08, R^* 0.66). This result stands in contrast with the synergies extracted from this frog with our algorithm, where both a synergy with RI and ST (synergy E), and a synergy with SM and VE (synergy D) are found (Fig. 8*C*). The difference in result between the two methods can be und erstood by considering which synergies are "sources" of RI, ST, SM, and VE, and how they are correlated.

RI and ST occur together in synergy E, but RI also occurs without ST in synergy B. However, B and E are positively correlated (Fig. 8*D*, $R\cdot$ 0.46, $R\square$ 0.67, R^* 0.88), and thus RI and ST remain positively correlated.

SM and VE occur together in synergy D, but SM also occurs without VE in synergy B. In this case, however, B and D are negatively correlated (Fig. 8*E*, $R\cdot$ −0.27, $R\square$ −0.89, R^* −0.82). As D increases, VE increases, but because of the B-D negative correlation, the increase in the D-source of SM tends to be offset by a decrease in the B-source of SM, so that SM may not increase concomitantly with VE. Thus SM and VE

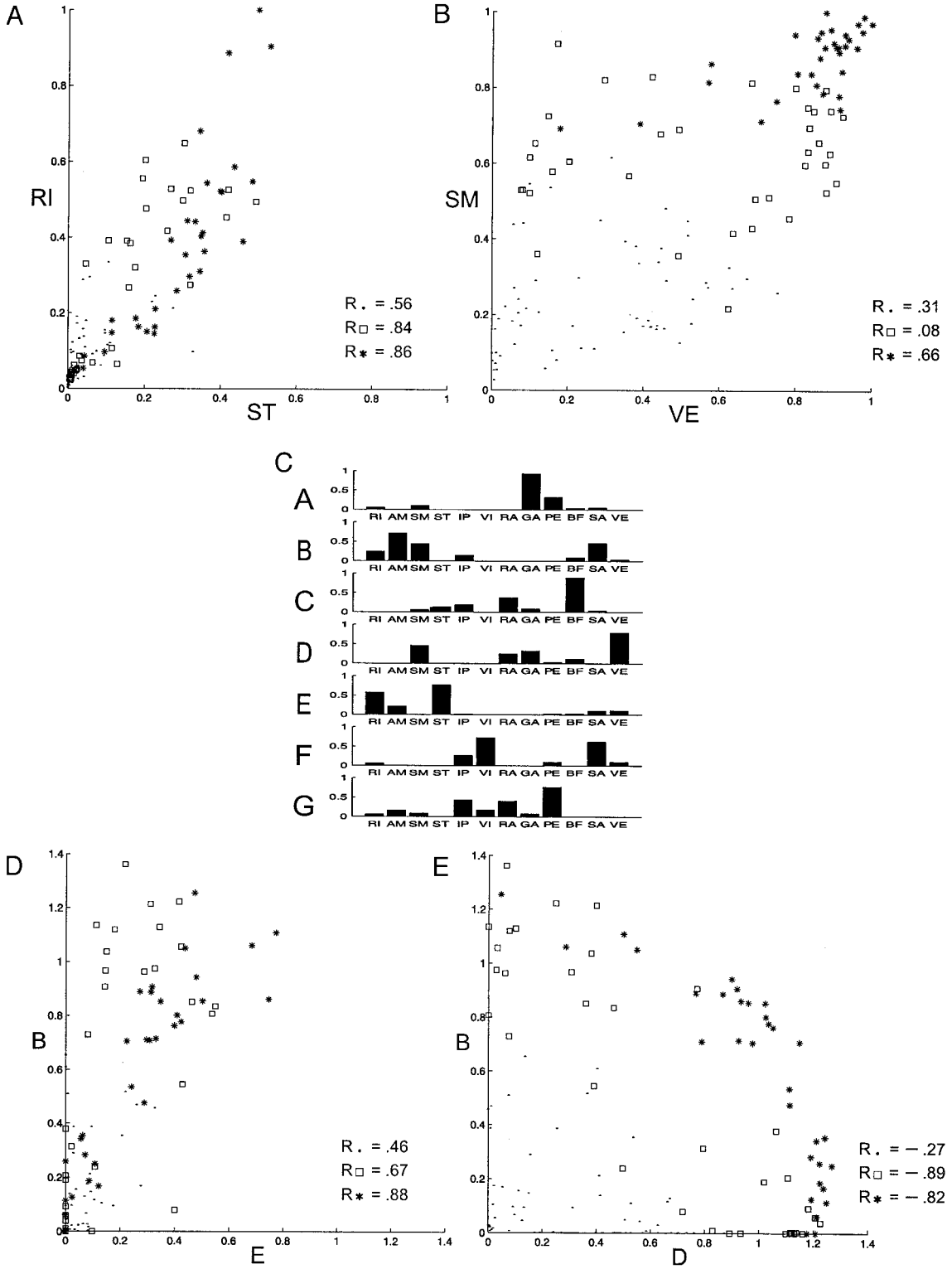

FIG. 8. Contrast with another method of identifying synergies. *A* and *B*: the activation levels of RI vs. ST, and SM vs. VE plotted for caudal extension EMG responses ($n = 129$) obtained from a single spinal cord site from the same frog as Figs. 6 and 7. The responses are divided in 3 groups of EMG magnitude (labeled ·, □, and * from weakest to strongest), and the correlation coefficients are indicated for each group. *C*: the 7 synergies extracted from the entire set of responses ($n = 361$) from this frog (*F149*). By matching these with the 7 synergies from the pooled data (Fig. 2*B*), the synergies A to G are identified. Synergies B, D, and E are the most relevant to the muscles plotted in *A* and *B*. *D* and *E*: the activation levels of synergy B vs. E, and synergy B vs. D plotted for the same responses studied in *A* and *B*. The correlation coefficients are indicated.

appear poorly correlated, when plotted one against another. The SM, VE synergy fails to be recognized.

In summary, the fact that many muscles belong to more than one synergy may explain the difficulty in their identification by techniques that compare the activity or the tuning curves of pairs of muscles.

The other major result is the identification of preferred synergy combinations (Table 1). Since these combinations were found when the extracting algorithm had a smaller number of available synergies to still reconstruct the same EMG data as well as possible, one would expect these combinations to be of synergies that often occurred together (and co-varied) in the data. Evidence for this interpretation was provided by finding concordance with how the synergies correlated pair-wise as they reconstructed the EMG data, as evaluated both by rank-ordering these correlations (Fig. 5), or examining plots of the coefficients of activation of the synergies against one another (Fig. 6). Therefore it is highly likely that the identified preferred combinations are intimately related to the construction of the most frequently observed EMG patterns in the data. Given that the seven synergies of Fig. 2*B* are close to orthogonal (see above), the identification of preferred combinations is not a trivial consequence of small angular distances between some of the synergies.

Further support for the identified synergies and their preferred combinations is that they can be recognized on visual inspection of the data. For example, the EMGs at the onset and end of Fig. 1*C* correspond to synergy E (Fig. 2*B*). The C + D + G triplet, a common combination, largely accounts for the EMGs of *phase 1* in Fig. 1, as shown in the coefficients of reconstruction in Fig. 3*C*. Furthermore, addition of the B + E pair largely accounts for the change from *phase 1* to *2*, and is also an important element of the change from *phase 3* to *4*. Phasic activations of the A + D, C + D + G, B + E, or F + G combinations can also be appreciated in Fig. 7. In fact, as indicated earlier, it was the evidence derived from visual inspection of smaller embedded synergies within the observed EMG patterns that motivated to an important degree the development and application of our extracting algorithm.

In summary, a small set of synergies, similar between frogs, is able to account, through preferred linear combinations, for a large repertoire of motor output derived from direct interneuronal stimulation of the spinal cord. It is suggested that these synergies will be useful to study how the spinal cord constructs the EMG sequences associated with the force directions of different phases of specific classes of rhythms, and to examine for possible linkages between these phases.

This research was supported by National Institute of Neurological Disorders and Stroke Grant NS-09343 to E. Bizzi. K. Wyler-Duda was supported by the Novartis Foundation and the Swiss Foundation for Medical-Biological Grants. M. C. Tresch was supported by a Howard Hughes Medical Institute predoctoral fellowship.

REFERENCES

BERKINBLIT MB, FELDMAN AG, AND FUKSON OI. Adaptability of innate motor patterns and motor control mechanisms. *Behav Brain Sci* 9: 585–638, 1986.

BERNSTEIN N. *The Coordination and Regulation of Movements.* Oxford, UK: Pergamon, 1967.

BIZZI E, MUSSA-IVALDI FA, AND GISZTER SF. Computations underlying the execution of movement: a biological perspective. *Science* 253: 287–291, 1991.

BUFORD JA AND SMITH JL. Adaptive control for backward quadrupedal walking. II. Hindlimb muscle synergies. *J Neurophysiol* 64: 756–766, 1990.

COCHILLA AJ AND ALFORD S. NMDA receptor–mediated control of presynaptic calcium and neurotransmitter release. *J Neurosci* 19: 193–205, 1999.

DELIAGINA TG, ORLOVSKY GN, AND PERRET C. Efferent activity during fictitious scratch reflex in the cat. *J Neurophysiol* 45: 595–604, 1981.

FIELD EC AND STEIN PSG. Spinal cord coordination of hindlimb movements in the turtle: intralimb temporal relationships during scratching and swimming. *J Neurophysiol* 78: 1394–1403, 1997.

FLANDERS M. Temporal patterns of muscle activation for arm movements in three-dimensional space. *J Neurosci* 11: 2680–2693, 1991.

GISZTER SF, MUSSA-IVALDI FA, AND BIZZI E. Convergent force fields organized in the frog's spinal cord. *J Neurosci* 13: 467–491, 1993.

GRASSO R, BIANCHI L, AND LACQUANITI F. Motor patterns for human gait: backward versus forward locomotion. *J Neurophysiol* 80: 1868–1885, 1998.

GRILLNER S. Control of locomotion in bipeds, tetrapods and fish. In: *Handbook of Physiology. The Nervous System. Motor Control.* Bethesda, MD: Am. Physiol. Soc., 1981, sect. 1, vol. II, p. 1179–1236.

HARTIGAN JA AND WONG MA. A k-means clustering algorithm. *Appl Stat* 28: 100–108, 1979.

HENRY SM, FUNG J, AND HORAK FB. EMG responses to maintain stance during multidirectional surface translations. *J Neurophysiol* 80: 1939–1950, 1998.

HEPP-REYMOND M-C, HUESLER EJ, AND MAIER MA. Precision grip in humans. Temporal and spatial synergies. In: *Hand and Brain: The Neurophysiology and Psychology of Hand Movements*, edited by Wing AM, Haggard P, and Flanagan JR. San Diego, CA: Academic, 1996, p. 37–68.

JACOBS R AND MACPHERSON JM. Two functional muscle groupings during postural equilibrium tasks in standing cats. *J Neurophysiol* 76: 2402–2411, 1996.

KARGO WJ AND GISZTER SF. Rapid correction of aimed movements by summation of force-field primitives. *J Neurosci* 20: 409–426, 2000.

LABELLA LA, KEHLER JP, AND MCCREA DA. A differential synaptic input to the motor nuclei of triceps surae from the caudal and lateral sural cutaneous nerves. *J Neurophysiol* 61: 291–301, 1989.

LACQUANITI F AND SOECHTING JF. Coordination of arm and wrist motion during a reaching task. *J Neurosci* 2: 399–408, 1982.

LAWSON CL AND HANSON RJ. *Solving Least Squares Problems.* Englewood Cliffs, NJ: Prentice-Hall, 1974.

LIU H, WANG H, SHENG M, JAN LY, JAN YN, AND BASBAUM AI. Evidence for presynaptic N-methyl-D-aspartate autoreceptors in the spinal cord dorsal horn. *Proc Natl Acad Sci USA* 91: 8383–8387, 1994.

LOEB EP, GISZTER SF, SALTIEL P, MUSSA-IVALDI FA, AND BIZZI E. Output units of motor behavior: an experimental and modeling study. *J Cognit Neurosci* 12: 78–97, 2000.

MACPHERSON JM. Strategies that simplify the control of quadrupedal stance. II. Electromyographic activity. *J Neurophysiol* 60: 218–231, 1988.

MCCLELLAN AD AND FAREL PB. Pharmacological activation of locomotor patterns in larval and adult frog spinal cords. *Brain Res* 332: 119–130, 1985.

MUSSA-IVALDI FA, GISZTER SF, AND BIZZI E. Linear combinations of primitives in vertebrate motor control. *Proc Natl Acad Sci USA* 91: 7534–7538, 1994.

NICHOLS TR. A biomechanical perspective on spinal mechanisms of coordinated muscular action: an architecture principle. *Acta Anat* 151: 1–13, 1994.

PEARSON KG AND ROSSIGNOL S. Fictive motor patterns in chronic spinal cats. *J Neurophysiol* 66: 1874–1887, 1991.

RAASCH CC AND ZAJAC FE. Locomotor strategy for pedaling: muscle groups and biomechanical functions. *J Neurophysiol* 82: 515–525, 1999.

SALTIEL P, TRESCH MC, AND BIZZI E. Spinal cord modular organization and rhythm generation: an NMDA iontophoretic study in the frog. *J Neurophysiol* 80: 2323–2339, 1998.

SANTELLO M, FLANDERS M, AND SOECHTING JF. Postural hand synergies for tool use. *J Neurosci* 18: 10105–10115, 1998.

SHERRINGTON CS. Flexion reflex of the limb, crossed extension reflex, and reflex stepping and standing. *J Physiol (Lond)* 40: 28–121, 1910.

SOECHTING JF AND LACQUANITI F. An assessment of the existence of muscle synergies during load perturbations and intentional movements of the human arm. *Exp Brain Res* 74: 535–548, 1989.

SOECHTING JF, LACQUANITI F, AND TERZUOLO CA. Coordination of arm movements in three-dimensional space: sensorimotor mapping during drawing movement. *Neuroscience* 17: 295–311, 1986.

TRESCH MC, SALTIEL P, AND BIZZI E. The construction of movement by the spinal cord. *Nature Neurosci* 2: 162–167, 1999.